Pattern Recognition Letters 123 (2019) 31–38

Contents lists available at ScienceDirect

Pattern Recognition Letters

journal homepage: www.elsevier.com/locate/patrec

A deep learning-shape driven level set synergism for pulmonary nodule segmentation ☆

Rukhmini Roy [a], Tapabrata Chakraborti [b], Ananda S. Chowdhury [a,*]

[a] Department of Electronics and Telecommunication Engineering, Jadavpur University, Kolkata 700032, India
[b] Department of Computer Science, University of Otago, Dunedin 9016, New Zealand

ARTICLE INFO

Article history:
Received 18 September 2018
Available online 6 March 2019

Keywords:
Lung nodule segmentation
Level sets
Shape information
Convolutional neural networks

ABSTRACT

Accurate pulmonary nodule segmentation, an essential pre-requisite in every computer-aided diagnosis (CAD) system, significantly helps in the risk assessment of lung cancer. In this paper, we propose a synergistic combination of deep learning and shape driven level sets for automated and accurate lung nodule segmentation. A coarse-to-fine solution is adopted, where, a deep fully convolutional network is employed to obtain coarse segmentation. To achieve fine segmentation, shape driven evolution of level sets is designed. The seed points for initializing the level sets are obtained from the coarse segmentation of deep network in an automated manner. Perimeter and circularity of the evolving contours are employed for guiding the evolution of level sets. Experiments on the publicly available LIDC/IDRI dataset clearly reveal that our method outperforms several state-of-the-art competitors as well as its constituent parts, i.e., deep network and level set, when applied in isolation.

1. Introduction

Lung cancer is one of the largest causes of cancer related deaths worldwide. An estimated statistics states that every year 1.1 million people die due to lung cancer [1]. Lung nodules are the precursors of lung cancer. Early detection of lung nodule can increase the chance of survival. Computer aided diagnosis (CAD) systems can help radiologists to detect lung cancer in an early stage with the help of automated detection, segmentation and classification of lung nodules. Computed Tomography (CT) is mostly used imaging technique for diagnosis of lung related diseases [2]. Segmentation of lung nodules is a prerequisite step in every CAD system. This problem becomes extremely challenging due to several factors like low contrast of the images, presence of noise and other nodule-like structures, variability in shapes of the nodules and possibility of the nodules to be attached to pleural surface and vascular structures present in the lungs. Lung nodule segmentation has been a popular research problem and quite a few existing works are available.

Zhao et al. [3] proposed a nodule segmentation algorithm on helical CT images using density threshold, gradient strength and shape constraint of the nodule. This algorithm fails to segment nodules attached to pleural surface of the lung due to similar intensities. A semi-automatic lung nodule segmentation approach was proposed by Diciotti et al. [4] which uses the knowledge of the expert in a reproducible way. The main disadvantage of this method is that it requires considerable interactions from the user. Dehmeshki et al. [5] presented a pulmonary nodule segmentation algorithm including nodules with vascular and pleural attachment. This method is highly dependent on user input and huge number of parameters. Failing to tune the parameters will change the segmentation result. Tachibana et al. [6] proposed a lung nodule segmentation algorithm using multiple thresholds and template matching. Their method sometimes results in poor accuracy and low efficiency due to complex space transformation and dynamic programming. Kishore et al. [7] performed lung nodule detection by combining watershed transform with morphological region segmentation. Li et al. [8] proposed a selective nodule enhancement filter to enhance the nodule structures by dominating the presence of other anatomical structures. A weak-supervised pulmonary nodule segmentation method is proposed by Liu et al. [9] using a modified self-adaptive FCM algorithm. They have given two algorithms for lung nodule segmentation. The first algorithm is an unsupervised adaptive FCM technique, where, according to the spatial information and grayscale information, the modified FCM function updates the fuzzy membership degree of centre pixels during each iteration with higher speed. In this algorithm, the cluster centres are chosen randomly at the initial stage. This kind of initialization degrades the performance of unsupervised clustering when it is applied to unlabelled samples. To overcome this issue, they

☆ **Conflict of interest.** None.

* Corresponding author.
E-mail address: as.chowdhury@jadavpuruniversity.in (A.S. Chowdhury).

https://doi.org/10.1016/j.patrec.2019.03.004
0167-8655/

proposed a fast weak-supervised segmentation method by using a small amount of prior labelled information. This algorithm can estimate the intrinsic logical relationship between clusters and categories for unlabelled images. It then utilizes the modified particle swarm optimizer (PSOm) to obtain cluster centres embedded in the objective function of FCM and category index from new samples efficiently. However, their method lacks in performance in segmentation of tightly adhered nodules.

Now, we discuss some specific works on CT lung imaging which have used level sets. For example, Swierczynski et al. [10] presented a method for joint image segmentation and registration in lung CT images using level sets. Farag et al. [11] proposed a variational level set approach for lung nodule segmentation. A circular model as a shape prior is fused as a signed distance function. The method can overcome the problem of nodules attached to the lung walls and vessels using the prior shape model. However, the method lacks in automating the initialization process. A hybrid system for lung nodule segmentation was proposed by Messay et al. [12] where a model based technique was combined with a trained neural network for segmentation. However, the solution is semi-automatic, and the performance of the algorithm degrades with a decrease in user interactions. Farhangi et al. [13] proposed a 3D active contour segmentation based on sparse linear combination of training shapes for lung nodule segmentation. They presented a unified segmentation framework for all types of lung nodules. However, the framework does not always yield good accuracies.

In recent research works, powerful supervised techniques like deep convolutional neural networks are often integrated with traditional model based segmentation approaches. For example, Mukherjee et al. [14] proposed a novel solution for lung nodule segmentation using deep learned prior based graph cut. The method obtains information of the location of the object using deep learning and the graph cut method preserves morphological intricacies of the objects. Overall, although several methods have been proposed for lung nodule detection/segmentation, most of the methods are semi-automatic and involve user interaction for segmentation. Some of the methods fail to segment nodules attached to lung boundary (juxta-pleural) due to presence of structures having similar intensity as that of the nodules. In case of level set based segmentation, automatic initialization becomes a challenging task which most of the methods have failed to address. In this work, we propose a fully automated end-to-end vision system based on a combination of deep learning and shape information driven level sets for pulmonary nodule segmentation. The synergism of data-driven and model based strategies is more suitable for addressing the intricacies of segmenting morphologically elaborate objects such as pulmonary nodules. The proposed method mainly considers two types of nodules for segmentation i.e., solitary pulmonary nodules/isolated nodules and juxta-pleural nodules (nodules attached to the boundary of the lung). Accurate segmentation of juxtapleural nodules is challenging due to the fact that these nodules are difficult to differentiate from surrounding tissues. In particular, we apply convolutional neural net (CNN) using Segnet to automate, expedite and improve the accuracy of shape information driven level sets to achieve this goal. The proposed work focuses on 2D lung nodule segmentation due to the fact that 3D processing requires more training time and storage space. Also, variability in slice thickness may affect the 3D lung nodule segmentation [15] whereas 2D lung CT images are not influenced by slice thickness. Different stages of the lung nodule segmentation using the proposed method are shown in Fig. 1. From the application perspective, our contribution lies in accurate detection of two different types of lung nodules present in pulmonary CT scans, which can help in better diagnosis of lung cancer. Theoretically speaking, our contributions are the following:

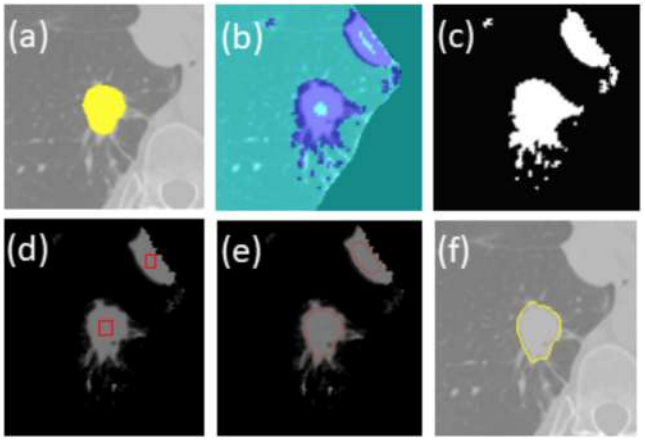

Fig. 1. Different stages of lung nodule segmentation using the proposed method. (a) Ground-truth (b) Segnet output (c) Segnet output label (d) Initial level set (e) Shape based level set evolution (f) Final output.

1. **Deep Learning-Level Set Synergism**: We propose a synergistic combination of a deep learning architecture, *i.e.*, Segnet with a classical computer vision technique, *i.e.*, level sets. Level set methods provide an accurate segmentation results but is sensitive to initialization, which is often done manually. In our approach, the coarse segmented output of the deep learning network is used to generate accurate seed points for the level sets without any manual intervention.
2. **Shape Driven Level Set**: A shape driven level set evolution algorithm is introduced. It mines the shape information of lung nodules in an automated fashion and sets the parameters of the level set. It up-weights circular and larger shapes as nodules are most likely to be circular in shape and larger in size, compared to artifacts and false-positive outliers. We use circularity and perimeter of the evolving contour to capture the nodule structures. Based on these two shape features, a weight function is incorporated within the area term of the level set method for accurate segmentation.

The rest of the paper is organized as follows. In Section 2, we present the proposed shape driven level set formulation and the deep learned fine tuned model. Section 3 presents the experimental setup, the results and analysis. The paper is concluded in Section 4.

2. Proposed methodology

In this section, we discuss in details different steps of the proposed method. The solution pipeline includes pre-processing followed by a synergistic combination of deep learning and shape driven level set evolution. The schematic of our proposed algorithm is presented in Fig. 2.

2.1. Pre-processing

The first step of the proposed algorithm is segmentation of lung field from CT scan images. The segmentation is performed using the algorithm proposed by Shen et al. [16]. It is a parameter-free lung segmentation algorithm to improve lung nodule detection accuracy focusing on juxta-pleural nodules. We choose this algorithm because it can take care of the segmentation of lung field including nodules attached to the lung boundary (juxta-pleural nodules). After lung segmentation, the images are re-sized to 128×128 to feed into deep learning network.

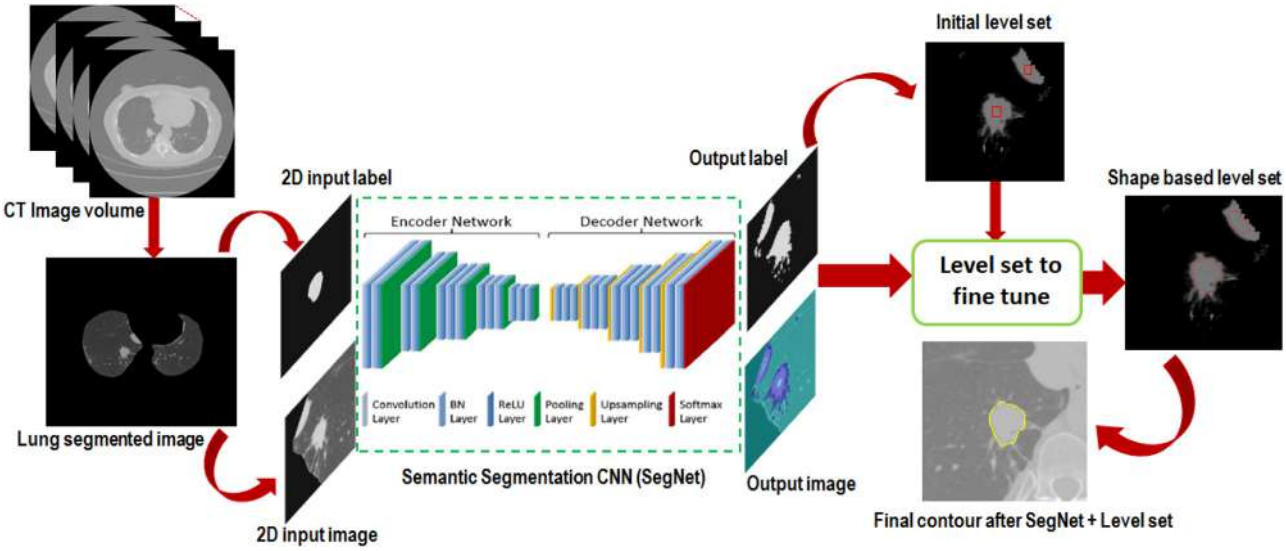

Fig. 2. Schematic diagram of the proposed method.

Table 1
Learning parameters for SegNet.

Parameters	Values
Momentum	0.9
InitialLearnRate	1e-3
L2Regularization	0.0005
MaxEpochs	100
MiniBatchSize	4
VerboseFrequency	2

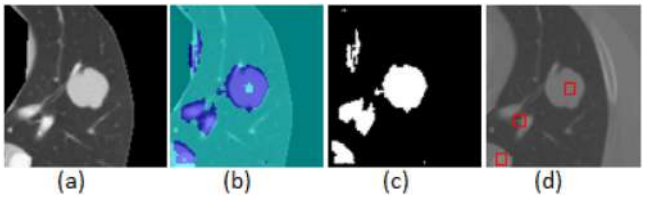

Fig. 3. Segnet results: (a) Input image (b) SegNet output (c) Labelled output (d) Initial level set.

2.2. Deep learning based coarse segmentation

We choose SegNet [17], a deep fully convolutional network architecture for coarse segmentation as it is specifically designed for pixel-wise semantic labelling. The deep network model SegNet is an encoder-decoder network. SegNet can provide a quick off-the-shelf segmentation solution for various applications in medical imaging [18,19]. Also, SegNet is easy to implement and has support from fast parallel computing method which improves the segmentation efficiency. In the training phase, a batch of 220 128×128 lung field images is used as input to the deep network. While training an estimated image is generated at the decoder end of the network. This generated image is then compared with the ground truth image to calculate the loss/error. The weights of the network are updated depending on the loss/error function. When the loss is minimum the final updated weights are used to get the segmented nodule image in the testing phase. A batch size of 4 is used over 220 images in the training phase which results in 55 iterations in 1 epoch of the network. Total 100 epochs are used to train the overall deep network. In the testing phase, the well-trained SegNet is used as a front-end segmentation classifier to segment test 2D images and generates coarse lung nodule segmentation from CT scan images. Different parameters for SegNet are mentioned in Table 1.

Coarse segmentation of lung nodules using SegNet results in some false positives. These false positives are removed at the next stage by the level set formulation. From the coarse segmentation of SegNet a centroid is obtained for each segmented object. Square boxes around the centroids are used for initializing the level sets. Fig. 3 shows the step-by-step results of the deep learned network. It illustrates how level sets are initialized from the SegNet output. Note that out of the three red squares, one is result of correct segmentation and two are generated due to false positive segmentation.

2.3. Shape driven level set for fine segmentation

The output of CNN initializes level set function for lung nodule segmentation. Different types of image information such as intensity, texture, shape can be used to define an objective function. The proposed algorithm employ shape information as the main image feature that drives the evolving contour to the desired object boundary. Let I be an image on a domain Ω, then the edge indicator function is defined by

$$g \triangleq \frac{1}{1 + |\nabla G_\sigma * I|^2} \tag{1}$$

where G_σ is a Gaussian kernel with a standard deviation σ and $*$ indicates convolution operation. For a level set function (LSF) ϕ, the energy function $\mathcal{E}(\phi)$ is defined by,

$$\mathcal{E}(\phi) = \mathcal{R}(\phi) + \mathcal{L}(\phi) + \alpha \mathcal{A}(\phi) \tag{2}$$

where $\alpha \in \Re$ is the co-efficient of the area term, $\mathcal{R}(\phi)$ is a distance regularization term as mentioned in [20], and $\mathcal{L}(\phi)$ and $\mathcal{A}(\phi)$ are the energy terms related to length and area respectively. The term $\mathcal{R}(\phi)$ is employed to maintain a desired shape of the level set function (LSF). The LSF tends to become too flat or too steep near the zero level set which results in numerical errors affecting the stability of the evolution [20]. The $\mathcal{L}(\phi)$ term is related to the energy along the length of the zero level contour ϕ. The $\mathcal{A}(\phi)$ term computes the energy inside contour, i.e., for the case where $\phi \geq 0$. The energy related to area speeds up the motion of the zero level contour which is required when the initial contour is placed far away from the desired object boundary. In our algorithm, the coefficient α takes negative value to expand the contour as the initial

contour is placed inside the object. The length and area terms of the i^{th} region are respectively defined by

$$\mathcal{L}_{\Omega_i}(\phi) = \int_{\Omega_i} g\delta(\phi)|\nabla\phi|dx \tag{3}$$

$$\mathcal{A}_{\Omega_i}(\phi) = \int_{\Omega_i} gH(\phi)dx \tag{4}$$

where the Dirac delta function δ computes a line integral of the edge indicator function g along zero level set ϕ. The Heaviside function computes the energy of the area inside the evolving contour. We now introduce a weight function in the area term of LSF according to the shape information of the nodule. As nodules are almost circular in shape and larger in size compared to other false positives, two features, namely, circularity and perimeter are used in LSF to improve nodule segmentation. The weight factor is incorporated into the area term due to the fact that it speeds up the curve evolution and our goal is to reach the boundary of a nodule faster than other nodule like structures or pathologies. The weight factor comprises of two terms which are defined as,

$$\mathcal{P}_i = \frac{\left[\mathcal{L}^4_{\Omega_i}(\phi)\right]}{\max\limits_{\forall\Omega_j}\left[\mathcal{L}^4_{\Omega_j}(\phi)\right]} \tag{5}$$

where P_i represents a normalized factor based on the perimeter of i^{th} region. The fourth power in P_i is used to better discriminate contours with larger perimeters over that of smaller ones. Circularity measures compactness of an object and is defined as:

$$\mathcal{C}_i = \frac{\mathcal{L}^2_{\Omega_i}}{4\pi\,\mathcal{A}_{\Omega_i}} \tag{6}$$

C_i is circularity of the contour with values in the range $1 < C_i < \infty$. An exact circular shape has circularity value of 1. A factor based on the circularity of the evolving contour for i^{th} region is formulated as

$$\gamma_i = \frac{1}{1+[1-e^{-(C_i-1)}]^2} \tag{7}$$

where $0 < e^{-(C_i-1)} < 1$ and $0.5 < \gamma_i < 1$. Now, the weight w_i^t is calculated from Eqs. (5) and (7) as

$$w_i^t = \mathcal{P}_i^{t-1} * \gamma_i^{t-1} \tag{8}$$

where t represents iteration. Area term after introducing weight factor becomes

$$\mathcal{A}_{\Omega_i}(\phi) = \int_{\Omega_i} gw_i H(\phi)dx \tag{9}$$

Now by replacing $\mathcal{A}_{\Omega_i}(\phi)$ in Eq. (2) with $\mathcal{A}_{\Omega_i}(\phi)$ as formulated in Eq. (9), the proposed energy function is defined as

$$\mathcal{E}(\phi) = \mu\int_{\Omega_i} p(|\nabla\phi|)dx + \int_{\Omega_i} g\delta(\phi)|\nabla\phi|dx + \alpha w_i\int_{\Omega_i} gH(\phi)dx \tag{10}$$

where $\mu > 0$ is a constant and $p(s) \triangleq \frac{1}{2}(s-1)^2$ is a potential or energy density function with a minimum point $s = 1$ that minimizes the distance regularization term $\mathcal{R}$ when $|\nabla(\phi)| = 1$ [20]. The energy function in Eq. (10) can be minimized by solving a gradient flow as,

$$\frac{\partial\phi}{\partial t} = \mu\,\mathbf{div}(d_p(|\nabla\phi|)\nabla\phi) + \delta(\phi)\mathbf{div}\left(g\frac{\nabla\phi}{|\nabla\phi|}\right) + \alpha w g\delta(\phi) \tag{11}$$

where d_p is a function using the first derivative of $p(s)$ as $d_p(s) \triangleq \frac{p'(s)}{s}$ [20]. The weight function w assigns different priorities to the object based on its shape. Fig. 4 shows the effect of weight function on different synthetic images. In both the images, we can see that the circular object gets priority over other objects due to factor related to circularity of evolving contour. Also, the factor related to perimeter of the evolving contour prioritizes the shape that is larger in size. Finally, both of these factors prioritize nodular structure over other objects as nodules are more circular and larger in size as shown in Fig. 5. The object that reaches to its boundary faster than other objects is selected as final nodule object. The proposed method is termed as deep learned shape driven level set (DLSDLSE) and the steps incorporated to develop the proposed method are shown in Algorithm 1.

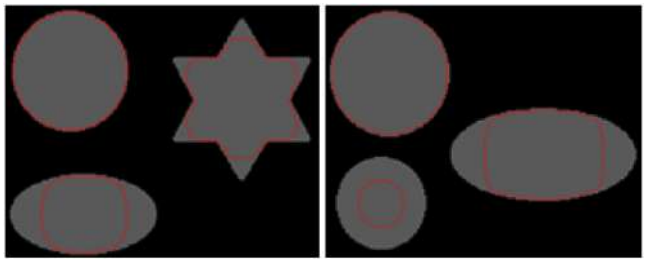

Fig. 4. Shape based level set on synthetic images.

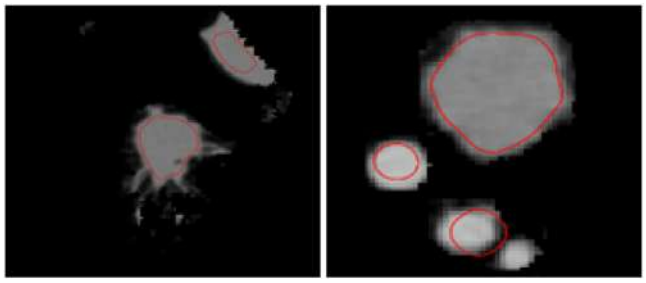

Fig. 5. Shape based level set on lung nodule images.

Algorithm 1 DLSDLSE Algorithm.

Input: Lung CT scans
Output: Segmented lung nodules

Parameter setting: $\alpha = -2.9$, ϵ = 0.005 ▷ α is the scaling factor and ϵ is the stopping factor
for $n = 1$ to N **do** ▷ N is the total number of CT scans
  Obtain segmented lung field from CT images
  Train CNN model using segmented lung field
  Generate R coarsely segmented nodule regions ▷ R represents number of regions
  Compute centroid for each regions
end for
for $t = 1$ to T **do** ▷ T represents number of iterations
  for $i = 1$ to R **do**
    Initialize $\phi_i^{Initial}$ at the centroid for i_{th} region ▷ $\phi_i^{Initial}$ is the initial level set
    Compute P_i based on Eq. 5
    Compute γ_i based on Eq. 7
    Update W_i based on Eq. 8
    Compute $A_{\Omega_i}(\phi)$ based on Eq. 9
    if $\frac{|\mathcal{A}^t_{\Omega_i}(\phi) - \mathcal{A}^{t-1}_{\Omega_i}(\phi)|}{\mathcal{A}^t_{\Omega_i}(\phi)} < \epsilon$ **then** $\phi_i^{Final} \longleftarrow \phi_i^t$ ▷ ϕ_i^{Final} is the final level set
    end if
  end for
end for

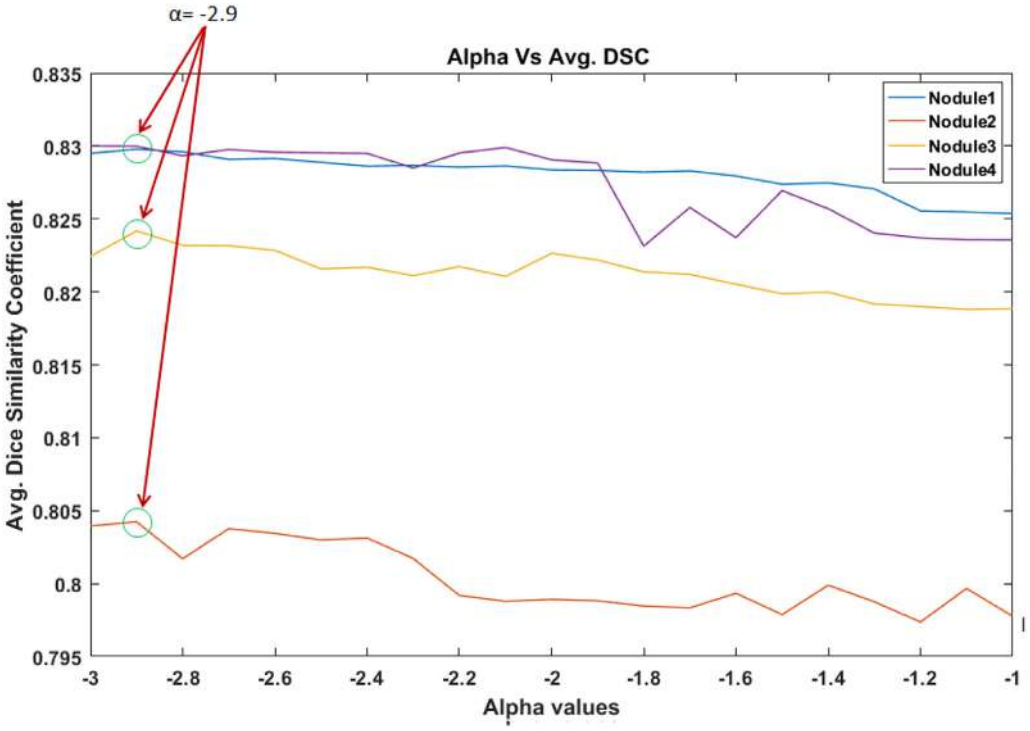

Fig. 6. Estimation of the scaling parameter alpha.

3. Experiments and results

In this section, we first describe the experimental conditions and the dataset used followed by performance measures. We then tabulate and analyze the results in details.

3.1. Dataset

A publicly available standard image dataset LIDC [21] is used for evaluation of the proposed lung nodule segmentation algorithm. The slices in this dataset are both low-dose and high-dose CT images as well as pre and post-intravenous (IV) in contrast. In LIDC-IDRI, each dataset is a breath-held CT image of the thorax with size 512×512. The number of slices vary between 95 and 672 and the in-plane pixel size varies between 0.5 and 0.8 mm/pixel. The range for the kVp for these data was 120–140 with 120 as the average and 20.99 as the standard deviation. The range for the mA was 30–634 with 215.9 as the average and 145.1 as the standard deviation. Four different radiologists annotated nodules that were greater than 3 mm in each scan. The deep neural network is trained on a set of 220 two dimensional axial slices for solid nodules and juxta-pleural nodules. The performance of the algorithm is evaluated on a separate test set consisting of 38 solid nodules and 25 juxta pleural nodules.

3.2. Performance measures

Two performance measures, namely, dice similarity co-efficient (DSC) and average error rate are used to compare the performance of the proposed algorithm with other methods. DSC measures the ratio between twice the number of elements common to two sets to the sum of number of elements in each set, i.e.,

$$DSC = \frac{2|A \cap B|}{|A| + |B|} \tag{12}$$

where A and B respectively denote the set representing the segmentation output of any algorithm and the ground truth, and $|.|$ denotes the cardinality of a set. The value of DSC is within the range [0, 1], where 1 indicates perfect overlap and 0 indicates no overlap between A and B. Average error rate $A(G_m, G_o)$ is defined as

$$A(G_m, G_o) = 1 - \frac{\int G_o \cap G_m dxdy}{\int G_o \cup G_m dxdy} \tag{13}$$

where, G_m represents the ground truth obtained from LIDC dataset and G_o refers to the segmentation result obtained from the proposed algorithm.

3.3. Parameter tuning

The parameter α is a scaling factor which controls the speed of the evolution of level set function. Fig. 6 shows the estimation of the parameter α for different 220 lung nodule images. It is clearly seen from Fig. 6 the proposed method achieves best result for $\alpha = -2.9$ over 220 lung nodule images. An example of 4 randomly selected different lung nodule images from these 220 images are shown in Fig. 6 for the estimation of the parameter α.

The boundary detection result for different values of parameter α is shown in Fig. 7. Note that, α is a scaling factor which represents the rate of evolution of the contour boundary. A large absolute value of α implies faster evolution of the level set with respect to number of iterations. It is seen that the segmentation is better with higher rate of evolution (optimal value of $\alpha = -2.9$). Along any column of the figure, with fixed number of iterations, performance gets better as $|\alpha|$ increases (1, 2 and 2.9). The three columns of the figure shows contour evolution at iterations 85, 135 and 185 respectively where the three rows represent α values at -1, -2 and -2.9 respectively. From the figure, it is clearly established that cases (g), (h), and (i) have achieved better segmentation in terms of dice similarity coefficient for optimal value of α (-2.9) as compared to cases with other α values.

Table 2
Dice Scores for Level Set based Algorithms.

Methods	Isolated nodule			Juxtapleural nodule		
	Min. DSC	Max. DSC	Mean ± std.	Min. DSC	Max. DSC	Mean ± std.
DRLSE [20]	0.33	0.93	0.89 ± 0.12	0.71	0.91	0.84 ± 0.09
WLSE [22]	0.78	0.94	0.91 ± 0.12	0.79	0.87	0.85 ± 0.08
SDLSE	**0.87**	**0.94**	**0.92 ± 0.11**	**0.81**	**0.93**	**0.89 ± 0.08**

Table 3
Dice scores for Ablation Study.

Methods	Isolated nodule			Juxtapleural nodule		
	Min. DSC	Max. DSC	Mean ± std.	Min. DSC	Max. DSC	Mean ± std.
SDLSE	0.87	0.94	0.92 ± 0.11	0.81	0.93	0.89 ± 0.08
SegNet	0.39	0.88	0.67 ± 0.13	0.21	0.85	0.58 ± 0.17
DL-SDLSE	**0.89**	**0.95**	**0.93 ± 0.11**	**0.88**	**0.97**	**0.9 ± 0.08**

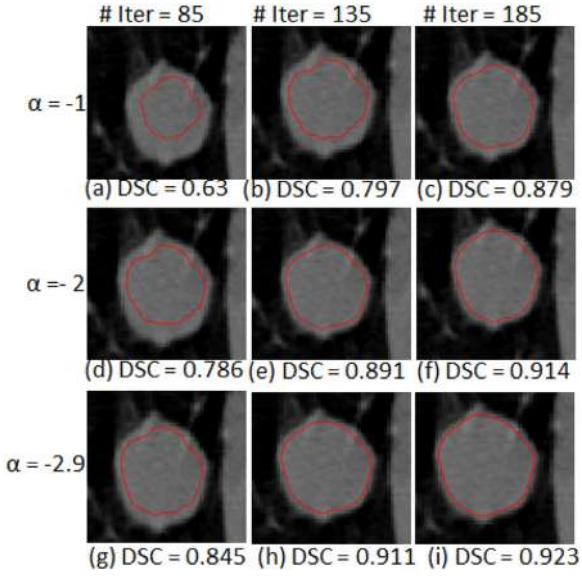

Fig. 7. Performance of the proposed method with different values for parameter α where three columns represent fixed iteration and three rows represent fixed α.

3.4. Comparison with other level set based approaches

The performance of the proposed shape based level set method (SDLSE) is compared with other level set approaches like distance regularized level set (DRLSE) [20] and a weight based level set method [22]. Dice similarity co-efficient (DSC) of two level set based algorithms DRLSE [20], WLSE [22] and proposed shape based level set are shown in Table 2. It can be stated from Table 2 that the proposed level set method outperforms other level set techniques even without using any learning.

3.5. Ablation study

Now, we compare different building blocks of the proposed algorithm. A qualitative analysis is also shown in Fig. 8. Table 3 compares the proposed method (deep learned (SegNet) shape data driven level set) DL-SDLSE with SegNet and shape driven level set (SDLSE) applied in isolation. Fig. 8 clearly portrays that DL-SDLSE performs better than SDLSE due to automated initialization of seed points obtained from Segnet. SDLSE is found to suffer from under-segmentation as the initial level set is generated manually whereas only Segnet results in oversegmented outputs. In addition, SDLSE takes 210 iterations to get the final nodule segmentation whereas DL-SDLSE takes 85 iterations to achieve the same.

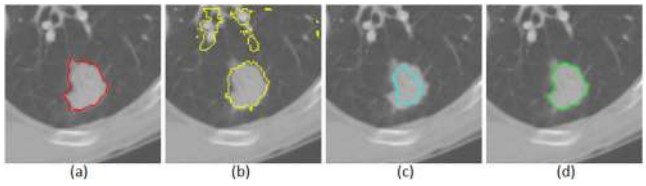

Fig. 8. (a) Ground truth (b) SegNet output (DSC = 0.67) (c) SDLSE output (DSC = 0.64) (d) DL-SDLSE output (DSC = 0.88).

Table 4
Error rate of nodule segmentation methods.

Algorithms	Error rate (%)	
	Isolated nodule	Pleural adhesion
Tachibana et al. [6]	0.28	0.40
Kishore et al. [7]	0.18	0.18
Dehmeshki et al. [5]	0.27	0.32
Li et al. [8]	0.23	0.20
Liu et al. (Self-adaptive FCM) [9]	0.21	0.27
Liu et al. (Fast weak-supervised segmentation) [9]	0.12	0.17
Proposed	**0.11**	**0.15**

Table 5
Dice scores for nodule segmentation methods.

Learning based algorithms	Isolated nodule		Pleura adhesion	
	Mean	Std.	Mean	Std.
DL-GC [14]	0.69	0.14	–	–
SCoTS [13]	0.75	0.14	0.64	0.20
U-Net [14]	0.57	0.24	–	–
Proposed	**0.93**	**0.11**	**0.9**	**0.08**

3.6. Comparison with additional nodule segmentation methods

The performance of the proposed segmentation algorithm is further compared with different existing methods of pulmonary nodule segmentation. These results are shown in Table 4 and in Table 5.

Table 4 clearly demonstrates that our method outperforms all other methods in terms of average error rate. Our method yields an 8.33% reduced error rate for isolated nodules and 11.76% reduced error rate for pleural adhesion nodules in terms of average error rate as compared to the fast weak-supervised segmentation algorithm [9]. Comparison of different learning based algorithms

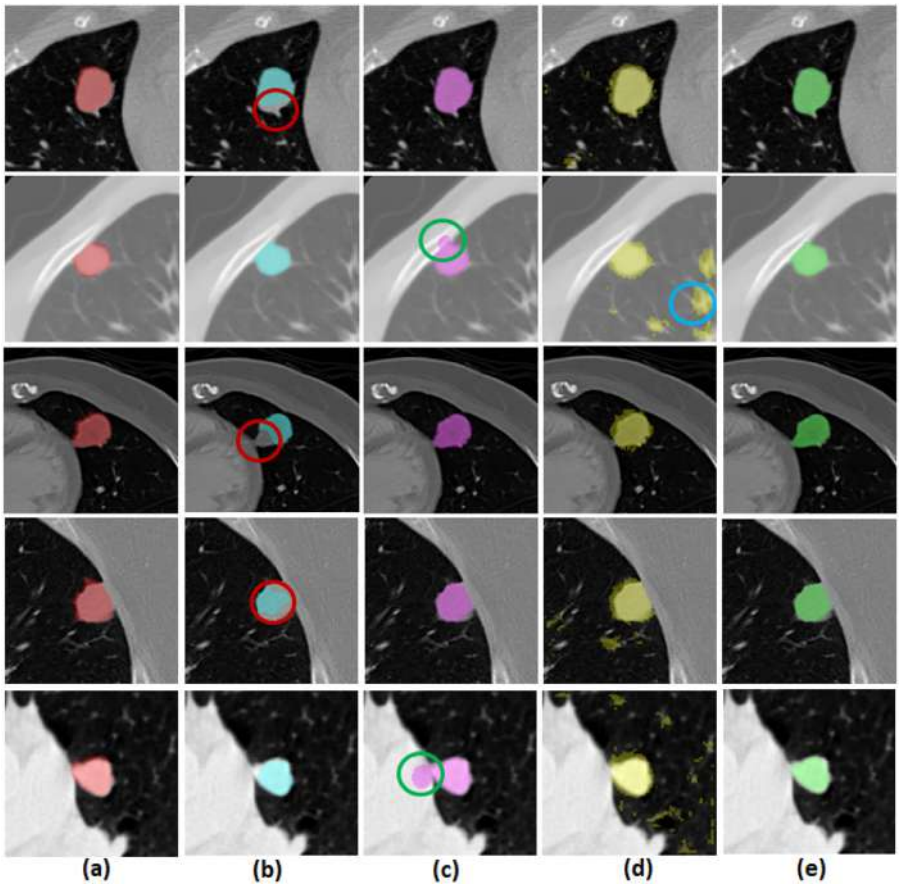

Fig. 9. Segmentation results (a) Ground truth (b) DRLSE (c) WLSE (d) SegNet (e) Proposed, red circle represents undersegmentation, green circle represents over segmentation and blue circle represents false segmentation. (For interpretation of the references to colour in this figure legend, the reader is referred to the web version of this article.)

with proposed method in terms of dice score is shown in Table 5. The proposed method performs better compared to other methods due to the fact that a coarse to fine segmentation approach is adopted by the synergy of deep learning and shape driven level set method. The deep network yields coarse segmentation which helps in better initialization of level set technique. The accurate seed point initialization in level set without any manual intervention helps in better automated segmentation of lung nodules. In case of DL-GC [14] the algorithm assumes an initial location of the nodule for segmentation which makes the method perform below par compared to the proposed method. Also, the proposed method performs better compared to SCoTS [13] due to the fact that their method is trained over a shape prior which results in inaccurate segmentation of lung nodules for varying shapes. Failures mostly happen in situations where the nodules are attached to organs with similar HUs and at the same time the shape prior of the nodule cannot be sparsely reconstructed from the dictionary. As our method is trained over intensity of the lung nodule, it can handle this problem more effectively which results in better dice similarity score and average error rate as compared to other methods.

Fig. 9 shows visual results of different algorithms. It is shown in Fig. 9 that DRLSE suffers from under-segmentation in some cases whereas WLSE suffers from over-segmentation in some cases. Also, vanilla SegNet results in false segmentation on lung nodule images. The proposed method can take care of all these drawbacks of DRLSE, WLSE and SegNet. So, in terms of visual results also it can be stated that our method outperforms all other methods like DRLSE [20], WLSE [22] and SegNet [17].

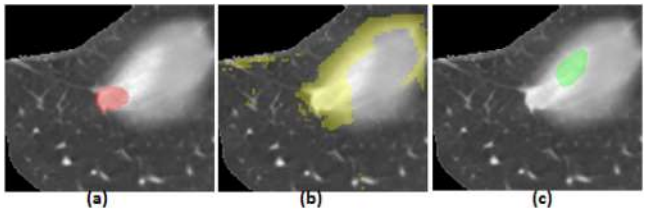

Fig. 10. Example of a failed case (a) Ground truth (b) SegNet (c) Proposed method.

Fig. 10 shows a failed segmentation result of the proposed algorithm. The algorithm fails in this case due to the fact that the CNN poorly segments the lung nodule as the nodule is partly occluded. This leads to erroneous initialization of level set resulting in improper nodule segmentation. In future, we are planning to handle this inaccurate segmentation with some modifications in the deep network architecture.

3.7. Execution time

The methods are implemented in Matlab 2017b and are executed on a windows 10 based computer with Intel(R) Core (TM) i7 CPU, with 16 GB RAM and 2.81 GHz clock speed. The time required by CPU to train CNN is 982 s over 220 images. The time required by DRLSE, WLSE and the proposed shape driven level set algorithm are 418 s, 532 s and 456 s respectively. Although the proposed level set method takes larger time than DRLSE, the accuracy of the proposed method is higher than that of DRLSE.

4. Conclusion

We present an end-to-end vision system for automated segmentation of pulmonary nodules from CT images using the synergism of deep learning and shape driven level sets. Convolutional neural net generates a coarse segmentation which provides automated level set initialization. Shape information is extracted in an automated manner to drive the level set for achieving fine segmentation. Experimental results on the benchmark LIDC/IDRI dataset indicate the advantage of the proposed method over several of state-of-the-art competitors as well as the constituent parts (CNN and level set in isolation). In future, we plan to enhance the proposed formalism to segment other types of lung nodules.

References

[1] A.L. Association, et al., Lung cancer fact sheet, 12, 2014. Accessed August
[2] M. Puderbach, H.-U. Kauczor, Can lung mr replace lung ct? Pediatr. Radiol. 38 (3) (2008) 439–451.
[3] B. Zhao, D. Yankelevitz, A. Reeves, C. Henschke, Two-dimensional multi-criterion segmentation of pulmonary nodules on helical ct images, Med. Phys. 26 (6) (1999) 889–895.
[4] S. Diciotti, G. Picozzi, M. Falchini, M. Mascalchi, N. Villari, G. Valli, 3-D segmentation algorithm of small lung nodules in spiral ct images, IEEE Trans. Inf. Technol. Biomed. 12 (1) (2008) 7–19.
[5] J. Dehmeshki, H. Amin, M. Valdivieso, X. Ye, et al., Segmentation of pulmonary nodules in thoracic CT scans: a region growing approach, IEEE Trans. Med. Imaging 27 (4) (2008) 467–480.
[6] R. Tachibana, S. Kido, Automatic segmentation of pulmonary nodules on CT images by use of NCI lung image database consortium, in: Medical Imaging 2006: Image Processing, vol. 6144, International Society for Optics and Photonics, 2006, p. 61440M.
[7] V.V. Kishore, R. Satyanarayana, Performance evaluation of edge detectors-morphology based ROI segmentation and nodule detection from DICOM lung images in the noisy environment, in: Advance Computing Conference (IACC), 2013 IEEE 3rd International, IEEE, 2013, pp. 1131–1137.
[8] Q. Li, F. Li, K. Doi, Computerized detection of lung nodules in thin-section ct images by use of selective enhancement filters and an automated rule-based classifier, Acad. Radiol. 15 (2) (2008) 165–175.
[9] H. Liu, F. Geng, Q. Guo, C. Zhang, C. Zhang, A fast weak-supervised pulmonary nodule segmentation method based on modified self-adaptive FCM algorithm, Soft comput 22 (12) (2018) 3983–3995.
[10] P. Swierczynski, B.W. Papież, J.A. Schnabel, C. Macdonald, A level-set approach to joint image segmentation and registration with application to CT lung imaging, Comput. Med. Imaging Graph. 65 (2018) 58–68.
[11] A.A. Farag, H.E.A. El Munim, J.H. Graham, A.A. Farag, A novel approach for lung nodules segmentation in chest CT using level sets, IEEE Trans. Image Process. 22 (12) (2013) 5202–5213.
[12] T. Messay, R.C. Hardie, T.R. Tuinstra, Segmentation of pulmonary nodules in computed tomography using a regression neural network approach and its application to the lung image database consortium and image database resource initiative dataset, Med. Image Anal. 22 (1) (2015) 48–62.
[13] M.M. Farhangi, H. Frigui, A. Seow, A.A. Amini, 3-D active contour segmentation based on sparse linear combination of training shapes (scots), IEEE Trans. Med. Imaging 36 (11) (2017) 2239–2249.
[14] S. Mukherjee, X. Huang, R.R. Bhagalia, Lung nodule segmentation using deep learned prior based graph cut, in: Biomedical Imaging (ISBI 2017), 2017 IEEE 14th International Symposium on, IEEE, 2017, pp. 1205–1208.
[15] D.P. Naidich, A.A. Bankier, H. MacMahon, C.M. Schaefer-Prokop, M. Pistolesi, J.M. Goo, P. Macchiarini, J.D. Crapo, C.J. Herold, J.H. Austin, et al., Recommendations for the management of subsolid pulmonary nodules detected at ct: a statement from the Fleischner Society, Radiology 266 (1) (2013) 304–317.
[16] S. Shen, A.A. Bui, J. Cong, W. Hsu, An automated lung segmentation approach using bidirectional chain codes to improve nodule detection accuracy, Comput. Biol. Med. 57 (2015) 139–149.
[17] V. Badrinarayanan, A. Kendall, R. Cipolla, SegNet: a deep convolutional encoder-decoder architecture for image segmentation, arXiv preprint arXiv:1511.00561 (2015).
[18] F. Liu, Z. Zhou, H. Jang, A. Samsonov, G. Zhao, R. Kijowski, Deep convolutional neural network and 3d deformable approach for tissue segmentation in musculoskeletal magnetic resonance imaging, Magn. Reson. Med. 79 (4) (2018) 2379–2391.
[19] N. Ing, Z. Ma, J. Li, H. Salemi, C. Arnold, B.S. Knudsen, A. Gertych, Semantic segmentation for prostate cancer grading by convolutional neural networks, in: Medical Imaging 2018: Digital Pathology, vol. 10581, International Society for Optics and Photonics, 2018, p. 105811B.
[20] C. Li, C. Xu, C. Gui, M.D. Fox, Distance regularized level set evolution and its application to image segmentation, IEEE Trans. Image Process. 19 (12) (2010) 3243.
[21] S.G. Armato III, G. McLennan, M.F. McNitt-Gray, C.R. Meyer, D. Yankelevitz, D.R. Aberle, C.I. Henschke, E.A. Hoffman, E.A. Kazerooni, H. MacMahon, et al., Lung image database consortium: developing a resource for the medical imaging research community, Radiology 232 (3) (2004) 739–748.
[22] A. Khadidos, V. Sanchez, C.-T. Li, Weighted level set evolution based on local edge features for medical image segmentation, IEEE Trans. Image Process. 26 (4) (2017) 1979–1991.